

Supplementary Materials for

The Importance of Evaluating the Lot-to-Lot Batch Consistency of Commercial Multi-Walled Carbon Nanotube Products

Mai T. Huynh,¹ Jean Francois Veyan,² Hong Pham,¹ Raina Rahman,¹ Samad Yousuf,¹ Alexander Brown,¹ Jason Lin,¹ Kenneth J. Balkus, Jr.,¹ Shashini D. Diwakara,¹ Ronald A. Smaldone,¹ Bryanna LeGrand,¹ Carole Mikoryak,³ Rockford Draper,^{1,3} and Paul Pantano^{1*}

¹ Department of Chemistry and Biochemistry, The University of Texas at Dallas, 800 West Campbell Road, Richardson, Texas 75080-3021, USA

² Department of Materials Science and Engineering, The University of Texas at Dallas, 800 West Campbell Road, Richardson, Texas 75080-3021, USA

³ Department of Biological Sciences, The University of Texas at Dallas, 800 West Campbell Road, Richardson, Texas 75080-3021, USA

* Correspondence: pantano@utdallas.edu (P.P.)

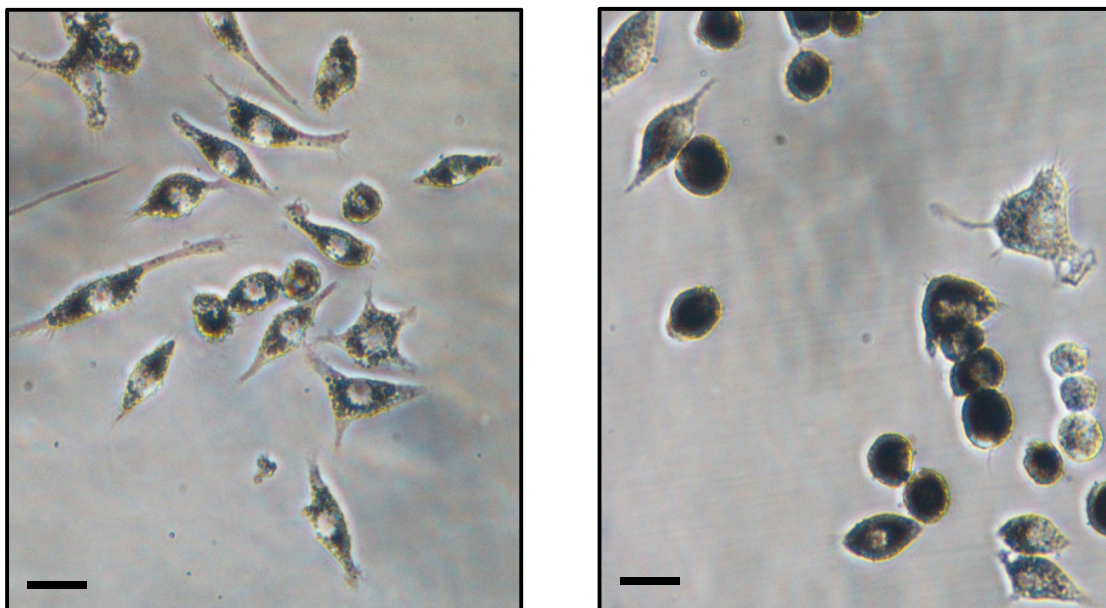


Figure S1. Representative phase contrast images acquired using an inverted light microscope (Nikon SMZ745T) equipped with a digital camera (Nikon DS-Fi2) of RAW 264.7 cells following 72 h of incubation with 125-µg/mL BSA-suspensions of 2015-pMWNTs (left) or 2018-pMWNTs (right). The scale bars represent 10 µm.

Table S1. ICP-MS analyses of pMWNT and cMWNT powders.

		2015-pMWNTs	2015-cMWNTs	2018-pMWNTs	2018-cMWNTs	MDL*
Aluminum	Al	35.622	7.103	11.496	7.953	0.012
Antimony	Sb	0.138	0.149	0.025	0.005	0.002
Arsenic	As	0.245	0.052	0.345	0.052	0.052
Barium	Ba	2.991	2.954	1.562	1.159	0.001
Beryllium	Be	0.014	0.014	0.014	0.014	0.014
Bismuth	Bi	0.003	0.001	0.022	0.470	0.001
Boron	B	14.625	18.884	9.189	10.957	0.174
Cadmium	Cd	0.029	0.004	0.005	0.008	0.004
Calcium	Ca	1,186.718	1,343.731	651.953	1,419.302	0.063
Chromium	Cr	8.932	0.837	3.714	18.656	0.005
Cobalt	Co	24.597	2.679	1,241.834	4.183	0.014
Copper	Cu	2.169	0.348	0.649	3.231	0.012
Gallium	Ga	0.026	0.005	0.015	0.012	0.005
Germanium	Ge	0.030	0.014	0.014	0.014	0.014
Gold	Au	0.003	0.003	0.003	0.003	0.003
Iron	Fe	1,689.820	28.690	475.353	123.964	0.022
Lead	Pb	0.543	0.033	0.076	0.721	0.005
Lithium	Li	0.130	0.085	0.092	0.055	0.001
Magnesium	Mg	197.304	198.221	66.185	174.402	0.002
Manganese	Mn	7.283	0.308	5.841	12.433	0.007
Molybdenum	Mo	110.852	4.300	3.237	9.936	0.009
Nickel	Ni	5,591.619	78.091	8.792	97.132	0.029
Niobium	Nb	0.189	0.012	0.008	0.007	0.002
Platinum	Pt	0.008	0.050	0.048	0.008	0.008
Potassium	K	20.245	30.789	13.715	33.888	0.021
Silver	Ag	1.675	0.318	0.009	0.014	0.003
Sodium	Na	78.042	72.556	31.502	49.317	0.004
Strontium	Sr	3.462	5.675	2.028	5.344	0.001
Tantalum	Ta	0.002	0.004	0.001	0.001	0.001
Thallium	Tl	0.001	0.001	0.001	0.001	0.001
Tin	Sn	0.147	0.035	0.145	0.179	0.003
Titanium	Ti	5.707	6.533	1.246	0.804	0.011
Tungsten	W	0.097	0.025	0.048	0.023	0.003
Vanadium	V	0.121	0.070	0.938	0.292	0.004
Zinc	Zn	10.458	2.308	1.314	2.965	0.018
Zirconium	Zr	16.233	479.190	119.315	42.038	0.010

* MDL = Method detection limit; MWNT data listed in blue font indicates that the observed results were at or below the MDL. All values are reported in units of ppm.

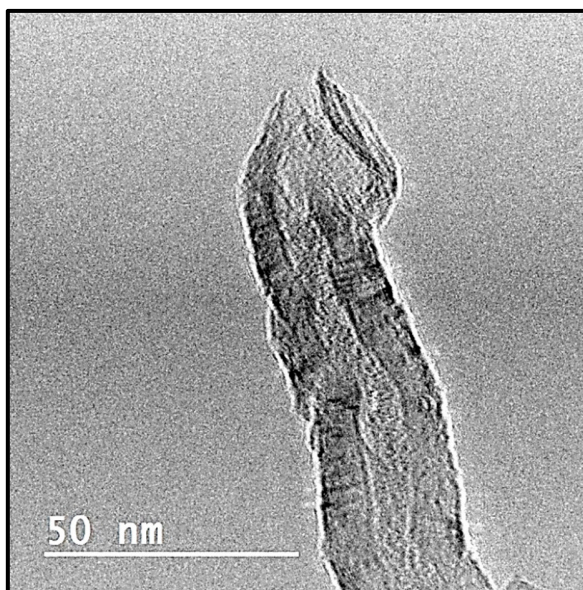


Figure S2. Representative HR-TEM image of a 2015-pMWNT highlighting asymmetric (bent) sidewall damage and a partially-collapsed, open-end.

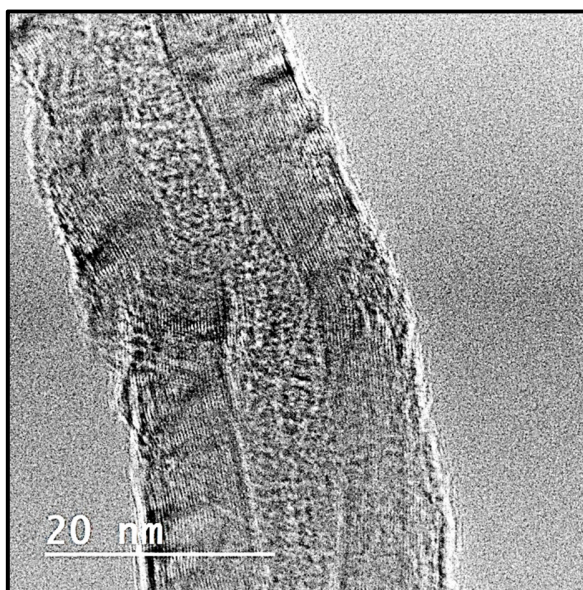


Figure S3. Representative HR-TEM image of a 2015-pMWNT showing asymmetric (bent) sidewall damage.

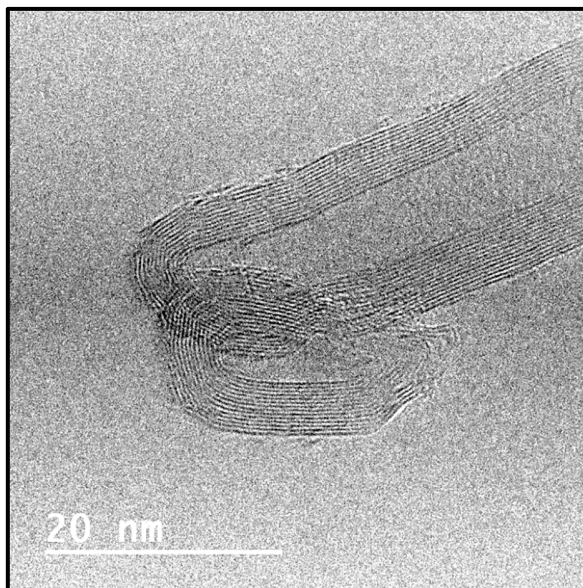


Figure S4. Representative HR-TEM image of a 2018-pMWNT highlighting a closed-end nanotube architecture, a hollow inner-cylinder, and a unique anomaly at the tip.

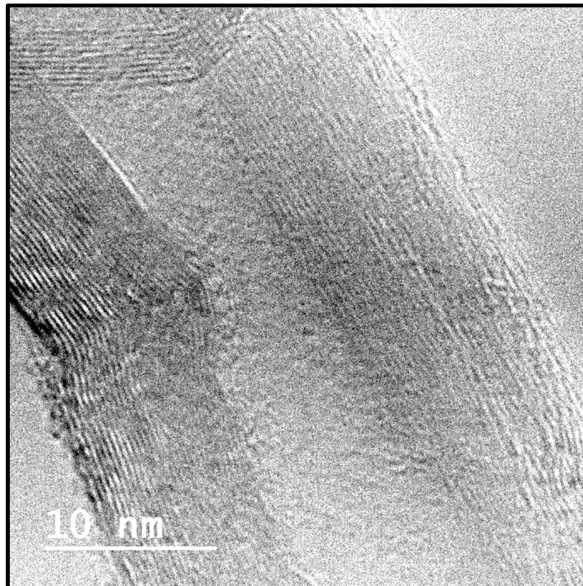


Figure S5. Representative HR-TEM image of a 2018-pMWNT highlighting asymmetric (bent) sidewall damage and sidewall debris.

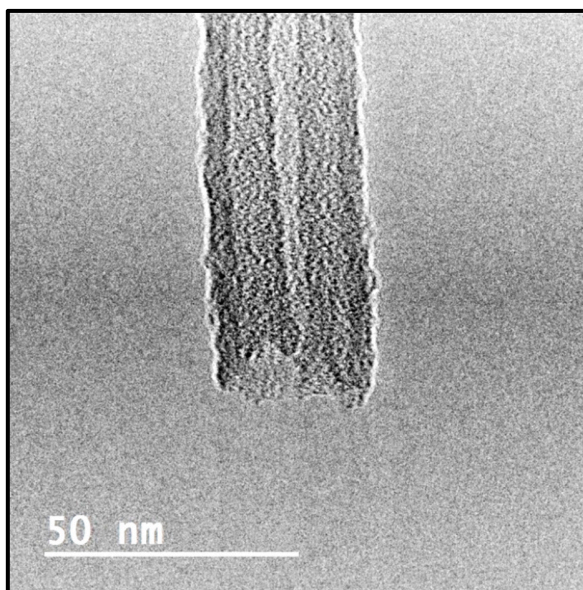


Figure S6. Representative HR-TEM image of a 2015-cMWNT highlighting a relatively symmetric, open-end nanotube architecture.

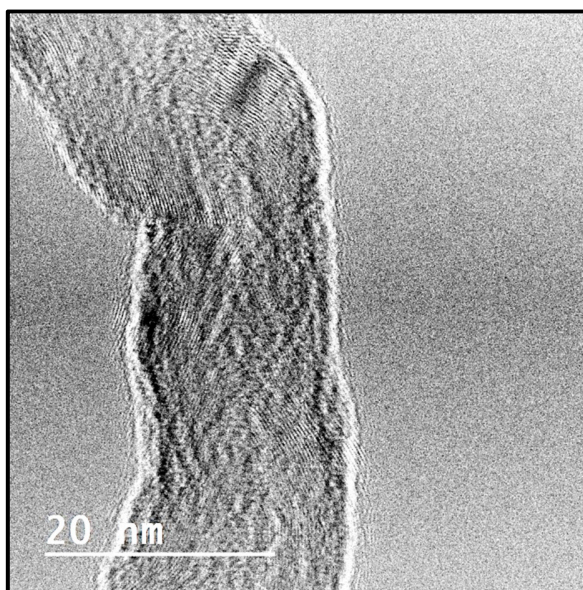


Figure S7. Representative HR-TEM image of a 2015-cMWNT highlighting asymmetric (bent) sidewall damage.

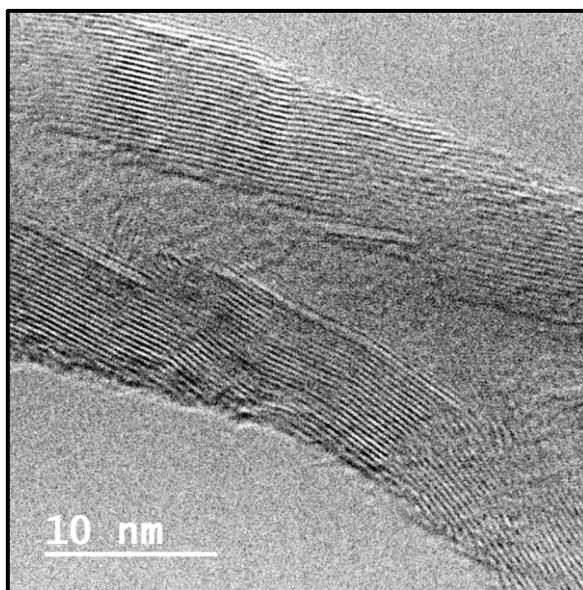


Figure S8. Representative HR-TEM image of a 2018-cMWNT highlighting a fishbone-type structure.

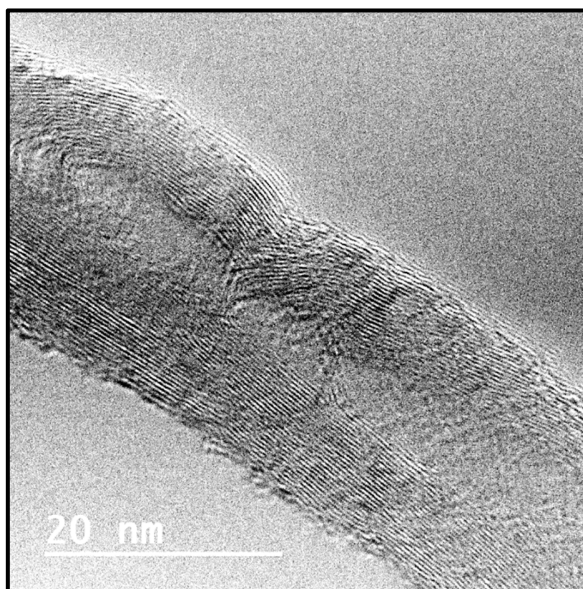


Figure S9. Representative HR-TEM image of a 2018-cMWNT highlighting cup-stacked structures.

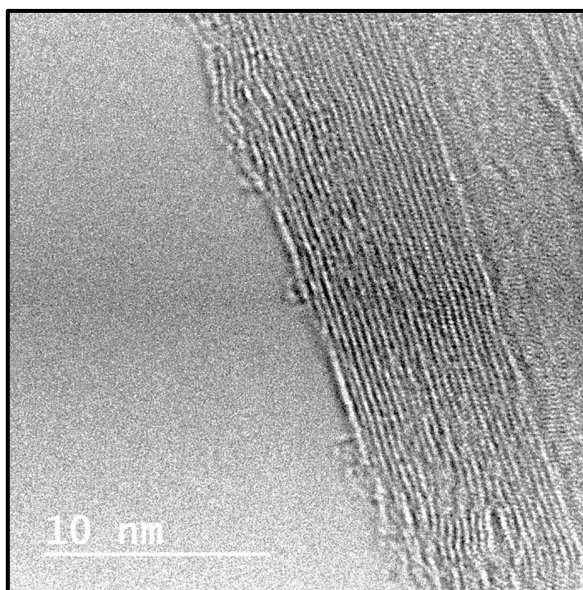


Figure S10. Representative HR-TEM image of a 2018-cMWNT highlighting a hollow inner-cylinder, sidewall damage, and sidewall debris.

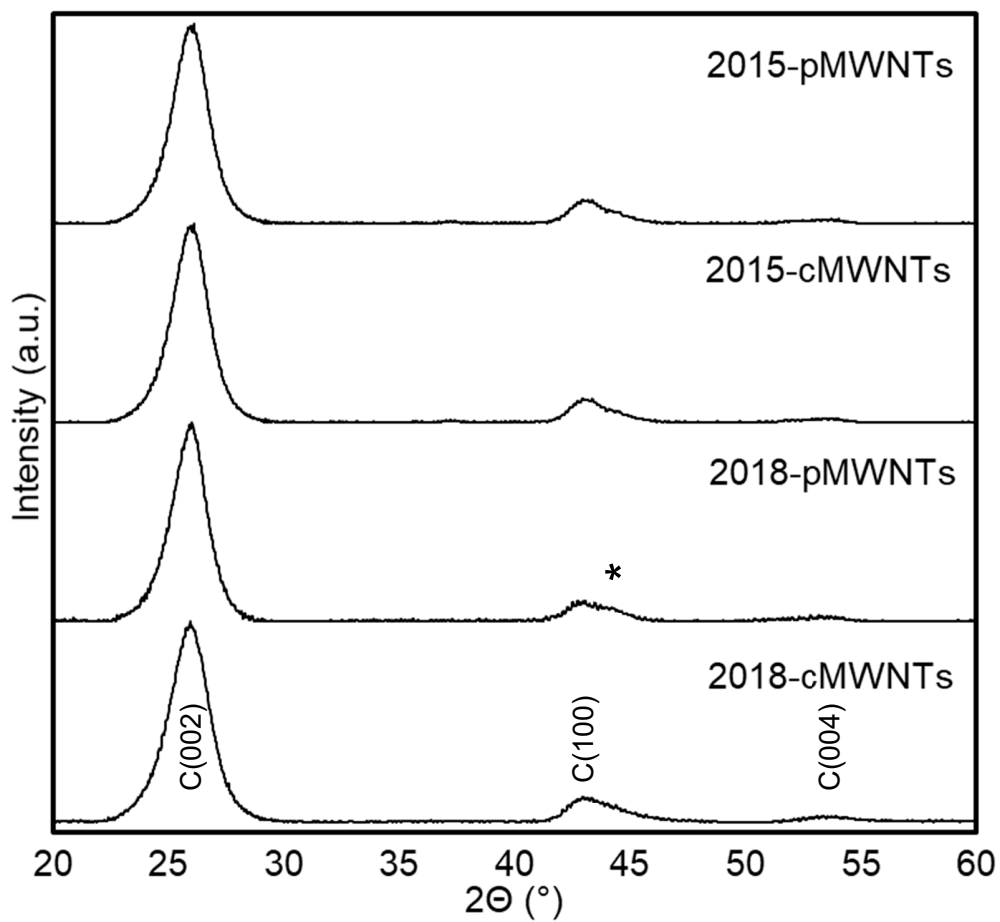


Figure S11. Representative XRD patterns (normalized and offset for clarity) of the 2015-pMWNT, 2015-cMWNT, 2018-pMWNT, and 2018-cMWNT powders showing the C(002), C(100), and C(004) diffraction peaks characteristic of an ideal graphite phase.

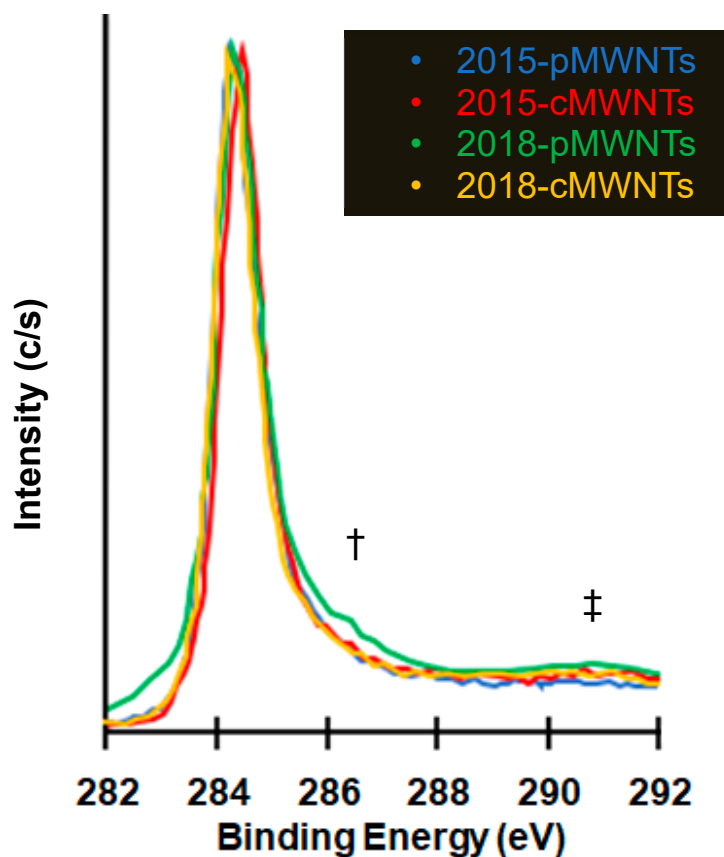


Figure S12. Representative C1s XPS spectra of the four MWNT powders where the major peak corresponds to sp^2 -hybridized carbons is centered: at 284.2 eV (FWHM \approx 1.1 eV) for the 2015-pMWNTs, at 284.4 eV (FWHM \approx 1.1 eV) for the 2015-cMWNTs, at 284.2 eV (FWHM \approx 1.1 eV) for the 2018-pMWNTs, and at 284.3 eV (FWHM \approx 0.9 eV) for the 2018-cMWNTs. Note, that the <0.2 eV-differences in the positions of the main C1s peaks were considered insignificant based on the instrument's energy resolution. The symbols represent C1s spectral regions associated with sp^3 -hybridized carbons (†) and the π - π^* electronic transition that is representative of disordered sp^2 carbons (‡); see text for details.

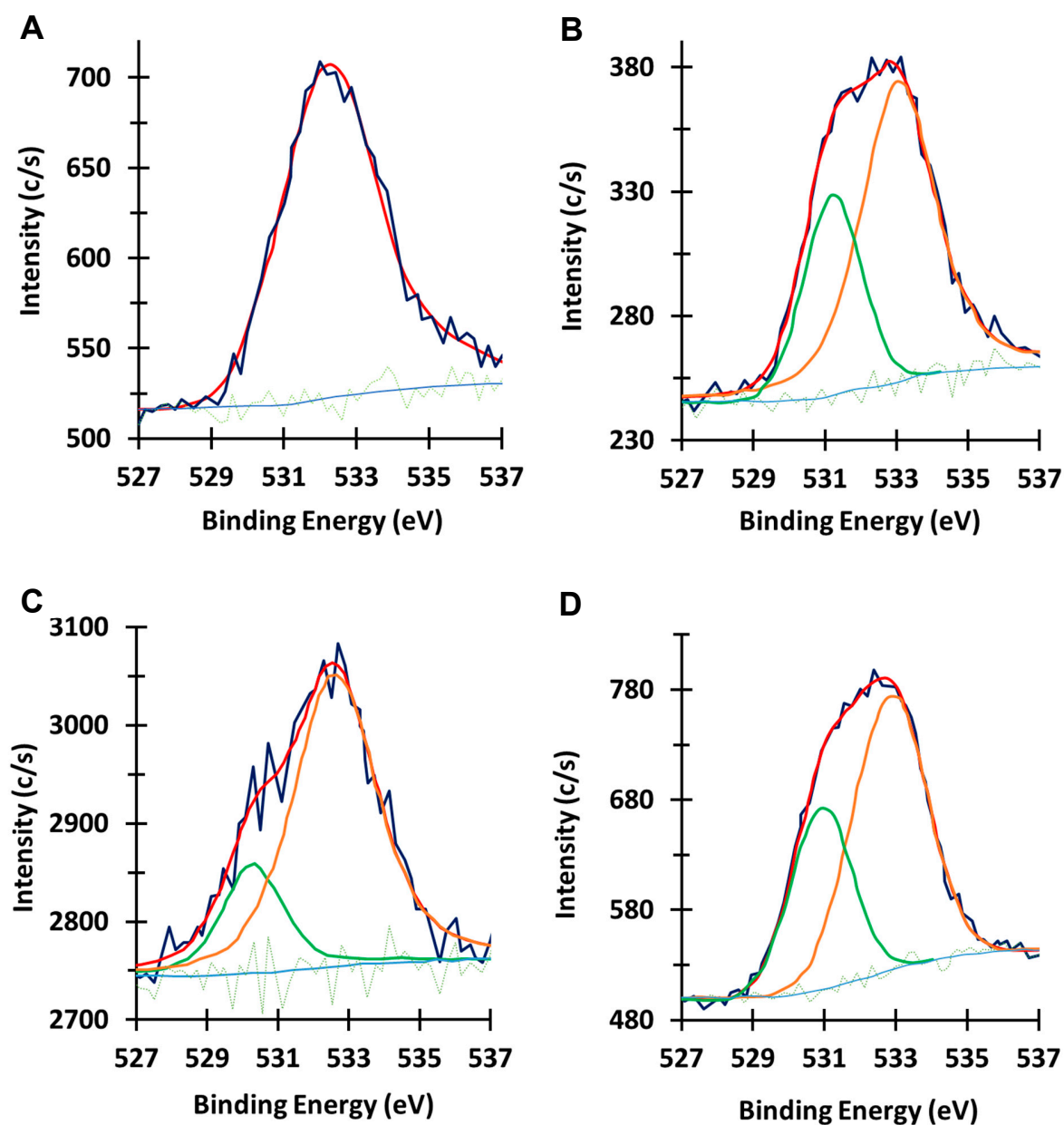


Figure S13. Representative O1s XPS spectra of (A) 2015-pMWNTs, (B) 2015-cMWNTs, (C) 2018-pMWNTs, and (D) 2018-cMWNTs. The dark-blue traces are the raw spectra and the red traces are the corresponding best fits; the light-green and light-blue traces are the raw background and smoothed background, respectively; and the green and orange traces are the best Gaussian fits.

Table S2. Analyses of the O1s XPS peaks from pMWNT and cMWNT powders.^a

MWNT Powder	Peak 1 Position (eV)	Peak 1 Area (%)	Peak 2 Position (eV)	Peak 2 Area (%)
2015-pMWNTs	532.14	100	----	----
2015-cMWNTs	533.09	70	531.25	30
2018-pMWNTs	532.67	78	530.37	22
2018-cMWNTs	532.86	65	530.94	35

^a Peak positions and areas determined from the O1s XPS peaks of the four MWNT powders shown in Figure S13. The O1s peak of the 2015-pMWNTs could be fit with a single Gaussian peak, while the O1s peaks of the other MWNT powders were best fit with two Gaussian peaks.